JBEP

Journal of Biosciences and Experimental Pharmacology
ISSN-2960-284X

Original Article

Effect of Selective COX-2 Inhibitor, Etoricoxib, on Inflammation and Oxidative Stress of Kidney and Heart in Two-Kidney, One Clip (2K1C) Rats

Shamima Sultana, Md. Haseebush Shaheed, Rahul Banik, Musfique Us Salehin, Sabrina Ahmed, Md Tayeb Hossen, Onika Zaman, Nusrat Subhan, Md Ashraful Alam*

Department of Pharmaceutical Sciences, North South University, Dhaka, Bangladesh

***Correspondence E-mail: ashraful.alam@northsouth.edu**

Citation: Shamima, S.; Shaheed, M. H.; Banik, R.; Salehin, M. S.; Ahmed, S.; Hossen, M. T.; Zaman, O.; Subhan, N.; Alam, M. A. Effect of Selective COX-2 Inhibitor, Etoricoxib, on Inflammation and Oxidative Stress of Kidney and Heart in Two-Kidney, One Clip (2K1C) Rats. *J. Bio. Exp. Pharm.* 2025, ***3(1)***, **24-55**

Academic Editor: Dr. Anayet Ullah

Received date: August 12, 2025
Accepted date: November 15, 2025
Published date: December 20, 2025

Publisher's Note: JBEP stays neutral with regard to jurisdictional claims in published maps and institutional affiliations.

Abstract: Oxidative stress and chronic inflammation may lead to chronic diseases like cancer, cardiovascular, and nephrological dysfunctions. Etoricoxib is used to treat pain and inflammation, which works by blocking the COX-2 enzyme selectively. This experiment was designed to investigate the effect of etoricoxib treatment on oxidative stress in the kidney and heart of 2K1C rats. Unilateral surgical stenosis of the renal artery [2-kidney-1-clip (2K1C) method] was performed on male Long Evans rats. These animals entered a 4-week dosing period with etoricoxib at a dose of 10mg/kg body weight/day through oral gavage. Blood plasma, heart, kidney, and liver tissues were collected and tested for the assessment of inflammation and oxidative stress in the kidney and heart of 2K1C rats after a 4-week experimental period. Biochemical measurement showed a significant increase in plasma AST, ALT, and ALP activity in 2K1C rats compared to the control rats, which was altered by etoricoxib treatment. Increased concentrations of oxidative stress markers, including malondialdehyde (MDA), nitric oxide (NO), and advanced protein oxidation product (APOP), were found in the plasma of 2K1C rats. The elevated levels of these oxidative stress markers were reduced by etoricoxib treatment. Furthermore, histopathological study revealed that 2K1C surgery also caused inflammatory cell infiltration and fibrosis in both heart and kidneys, which were further ameliorated by etoricoxib treatment. Our study suggests that etoricoxib treatment in 2K1C rats prevented inflammation and fibrosis of the heart and kidney by reducing elevated oxidative stress in heart and kidney tissues

Keywords: Etoricoxib, Fibrosis, Inflammation, Oxidative stress, Malondialdehyde

Introduction

Kidney disease is still a serious health condition in 2025, with its increasing prevalence and mortality rate worldwide. The global mortality rate from CKD climbed by 41.5% between 1990 and 2017 [1, 2]. Numerous other severe diseases, including diabetes, hypertension, cardiovascular problems, anemia, nerve damage, osteoporosis, hyperkalemia, and others, are linked to and can progress from kidney diseases [3]. The development of chronic kidney disease (CKD) is significantly influenced by chronic inflammation, which exacerbates kidney damage and reduces kidney function [4].

RAS, or the renin-angiotensin system, is a vital pathway connecting kidney function with the heart and blood vessels. Renin is an enzyme crucial for blood pressure regulation and is produced by the juxtaglomerular cells located in the wall of the afferent arterioles of the kidney [5]. Renin can directly cause vasoconstriction and also convert angiotensinogen to angiotensin I. It then transforms into angiotensin II, which also leads to vasoconstriction [6]. Angiotensin II is an important inflammatory mediator that can increase COX-2 expression and activate nuclear factor kappa B (NF-κB) in the cardiovascular and renal tissue [7]. When kidney injury occurs due to damage, stress, or renal artery stenosis, RAS can be overstimulated and can lead to renin overproduction, which can further damage the kidney [8]. Previous studies have reported that Angiotensin II increased cardiovascular tissue NADPH oxidase activity and stimulated production of reactive oxygen species (ROS) such as superoxide in the cardiovascular system [9]. Excessive production of the superoxide anion (O_2^-) can cause oxidative stress, lipid peroxidation, inflammation, and subsequent cardiovascular tissue injury [10].

On the other hand, RAS and COX-2 have a direct connection. The localized expression of inducible COX-2 in macula densa and the surrounding thick ascending limb of the kidney shows a relation between COX-2 and the renin-angiotensin system [11]. The macula densa is responsible for increased renin secretion, and an increased COX-2 can regulate the renin release via the production of prostaglandins [12, 13]. On the other hand, the renin-angiotensin

system can trigger the localized upregulation of COX-2 [14, 15]. Additionally, COX-2 can be upregulated and activated by ROS, and COX-2 itself can contribute to the generation of ROS. ROS can trigger COX-2 via several mechanisms, including NF-kB and MAPKs [16]. Additionally, COX-2 is linked to diabetic nephropathy, a condition in which the kidneys' overexpression of the protein causes albuminuria and glomerular damage. COX-2 selective inhibition hinders the progression of renal damage [17].

A widely used experimental model for creating a mimic of the pathophysiology of the kidney disease is the Goldblatt 2K1C (two-kidney, one-clip) rat model, which can activate RAS following inflammatory cascades and increase blood pressure [18]. 2K1C rat models are surgically created by clipping and constricting the blood flow through the renal artery of one kidney, leaving the other kidney intact. This constriction of blood flow will reduce renal perfusion and necessary oxygen and nutrient transfer, and ultimately, the kidney will be damaged [19]. This may also lead to renovascular hypertension, cardiovascular hypertrophy, electrolyte imbalance, fluid retention, creatinine and uric acid accumulation, etc. [20, 21].

Previous experimental data indicate that the COX-2 inhibitor Aspirin is a potent antioxidative agent that effectively reduced production of cardiovascular tissue superoxide, decreased hypertension, reinstated the vasodilation in spontaneously hypertensive rats [22] and thus prevented angiotensin II (Ang II)–induced oxidative stress, hypertension, and cardiovascular tissue hypertrophies [23].

Like Aspirin, Etoricoxib has been found to suppress oxidative stress due to experimental renal Ischemia/Reperfusion [24]. Again, in a recent study, etoricoxib has been reported to significantly prevent the rise of COX-2, MDA, and MPO and the decline of GSH and COX-1 in the ovarian tissue subjected to Ischemia/Reperfusion [25]. This information suggests that etoricoxib may be beneficial in preventing oxidative stress and inflammation. The present study was designed to determine whether the COX-2 selective NSAID etoricoxib can suppress oxidative stress and inflammation in the heart and kidney of two-kidney one-clip (2K1C) rats.

2. Materials and Methods

2.1 Chemicals and reagents

Etoricoxib was obtained from General Pharmaceuticals Limited (Bangladesh). Thiobarbituric acid (TBA) was purchased from Sigma Chemical Company (USA). Trichloroacetic acid (TCA) was purchased from J.I. Baker (USA). Alanine aminotransferase (ALT), aspartate aminotransferase (AST), alkaline phosphatase (ALP), and uric acid (UA) assay kits were obtained from DCI Diagnostics (Budapest, Hungary). All other chemicals and reagents used were of analytical grade.

2.2 Animal surgery and treatment

Twelve to fourteen weeks old, 24 Long Evans male rats (170–230 g) were obtained from Animal production unit of Animal House at Department of Pharmaceutical Sciences, North South University and were kept in ordinary cages at room temperature of 25 ± 3 °C with a 12 h dark/light cycles with food water ad libitum. They have free access to food and water, according to the study protocol approved by the Ethical Committee of the Department of Pharmaceutical Sciences, North South University, for animal care and experimentation. To study the effects of Etoricoxib, rats were equally divided into four groups (six rats in each group): Control, Control + Etoricoxib, 2K1C, and 2K1C + Etoricoxib.

Rats were subjected to unilateral clipping of the renal artery to produce two-kidney one-clip (2K1C) model rats. For the 2K1C surgery, rats were first anesthetized using 50mg/kg ketamine, and the left side of the abdomen, beside the spinal cord, was carefully shaved, cleared, and disinfected using ethanol. A small cut was made through the skin and muscle, and the left kidney was brought out of the cavity. The renal artery was then separated from the adjacent adipose tissue, ureter, and veins, and a 2-3mm long plastic tube with an internal diameter of 0.4mm was used to clip the artery. The tube was prepared from a butterfly needle, and to stabilize the position of the tube clip, it was knotted with a surgical thread. This clip was used to block the renal perfusion. After the clipping, the kidney was placed back inside the

peritoneal cavity, and the incision was closed up with surgical suture. The site was then cleaned with povidone iodine to avoid any infection. After the surgery, they were given time to heal for a few days and were kept under proper monitoring for their full recovery.

Control + Etoricoxib and 2K1C + Etoricoxib groups received Etoricoxib (10mg/ kg, daily) by oral gavage. After 28 days of the treatment, all the animals were weighed, sacrificed, and collected for the blood and organs like the heart, kidney, spleen, and liver. Immediately after the collection of these tissues and organs, they were weighed and stored at −20 °C for further analysis. Half of these organs were cut and kept in 10% formalin for histological analysis.

2.3 Plasma and Tissue Preparation

For the preparation of the plasma, the blood samples were collected in citrated buffer and centrifuged at 4000 rpm, 4°C for 15 minutes. After that, the plasma was collected using a micropipette.

For the tissue, an ultrasonic homogenizer was used to break down the cells in a finely dispersed, uniform condition to bring out the cellular contents outside of the cells. Phosphate buffer with pH 7.4 was used to homogenize the process, and after that, the uniform homogenized tissues were centrifuged at 8000 rpm, at 4°C for 15 minutes. The supernatants were collected and refrigerated for biochemical analysis.

2.4 Assessment of AST, ALT, and ALP activities

Liver marker enzymes (alanine aminotransferase (ALT), aspartate aminotransferase (AST), and alkaline phosphatase (ALP) were estimated in plasma by using Diatech diagnostic kits for AST, ALT, and ALP (Hungary) according to the manufacturer's protocol. 5µl of plasma or tissue homogenates were taken, and the reagents from the kits for each enzyme were added. After 1 minute, absorbance was taken at 405nm at 0 min, 1 min, 2 min, and 3 min.

2.5 Assessment of oxidative stress markers

For the analysis of oxidative stress markers, MDA, NO, and AOPP were estimated using plasma and tissue homogenates.

2.6 Estimation of lipid peroxidation product malondialdehyde (MDA)

Plasma concentrations of malondialdehyde are an index of lipid peroxidation and oxidative stress. Lipid peroxidation in the heart and kidney was estimated colorimetrically by measuring malondialdehyde, followed by the previously described method [26]. For plasma, 50µl, and tissue, 20µl homogenates were taken and mixed with phosphate buffer solution to add up to a volume of 100µl. After that, glacial acetic acid, thiobarbituric acid solution, and DMSO were added in an appropriate amount according to the protocol and heated for 10 minutes in a hot water bath. After cooling down to normal temperature, the absorbance was taken at 490nm two times.

2.7 Estimation of nitric oxide (NO)

NO was determined according to the method described by Tracy et al. as nitrate and nitrite [27, 28]. The Griess-Illosvoy reagent was modified by adding 0.1% w/v naphthyl ethylene diamine dihydrochloride in place of 5% 1-naphthyl amine. For plasma, 50µl and for tissue, 20 µl samples were taken, and phosphate buffer was added to make up to 100µl. The modified Griess-Illosvoy reagent was then added to the mixture, and after 15 minutes, the absorbance was measured at 490nm two times.

2.8 Estimation of advanced protein oxidation products (APOP)

Determination of APOP levels was performed by modification of the method of Witko-Sarsat [29] and Tiwari [30]. 10µl plasma or 5µl tissue homogenates were mixed with phosphate buffer solution, followed by the addition of 50µl acetic acid and 50µl KI solution [31]. After 2 minutes, absorbance was measured 2 times at 405nm. APOP concentrations were expressed as mmol/L chloramine-T equivalents.

2.9 Histopathological determination

For histopathological evaluation, heart and kidney tissues were kept in neutral buffered formalin. Tissues went through many procedures before being embedded in paraffin. After embedding, a 5 µm-thick slice of the paraffin-embedded tissue was cut and fixed onto a

histology slide, and subsequently stained with hematoxylin and eosin (H & E) and picrosirius red staining. After completion of the slide preparation, they were examined under a light microscope at 40× magnification.

2.10 Statistical analysis

The values are expressed as mean ± standard deviation (SD). The results were evaluated by using the Two-way ANOVA followed by the Bonferroni test using GraphPad Prism Software, USA, version 6. Statistical significance was considered as $p < 0.05$ in all cases.

2.11 Network pharmacology

2.11.1 Target Identification and Data Integration

The PubChem database was used to get the SMILES of the compound Hesperidin. SwissTargetPrediction (https://www.swisstargetprediction.ch/), SuperPred (https://prediction.charite.de/), and TargetNet (http://targetnet.scbdd.com/) were used to derive the target of the compound. Genes associated with "chronic kidney disease" were collected form Genecards databases. All gene names were standardized utilizing the UniProtKB database. Venny 2.1 (https://bioinfogp.cnb.csic.es/tools/venny/) was used to identify the overlapping genes.

2.11.2 PPI Network Construction and Topological Analysis

All intersected proteins were uploaded to the STRING database (https://string-db.org/). Organism was restricted to *Homo sapiens,* and the threshold was set to high confidence (>0.4). To analyze and visualize the complex merged network, we used Cytoscape 3.10.4. Topological parameters, including Degree, Betweenness Centrality (BC), and Closeness Centrality (CC), were calculated utilizing cytohubba plugins. The core bottleneck proteins influencing the network were identified using these metrics.

2.11.3 Functional Enrichment Analysis

Functional enrichment was carried out using a combination of platforms. ShinyGO (v0.80) provided Gene Ontology (GO) and Kyoto Encyclopedia of Genes and Genomes (KEGG) pathway analyses, with pathway diagrams retrieved using the KEGG API. Metascape was

applied for further GO enrichment and to explore disease associations through integration with DisGeNET. An adjusted *p*-value <0.05 was considered statistically significant for all tests.

2.12 Molecular Docking

2.12.1 Protein Preparation

Proteins were downloaded from the Protein Data Bank website (https://www.rcsb.org/) in PDB format. The downloaded proteins were: AKT1 (4EJN), APP (1AAP), CREBP (4TQN), FYN (2DQ7), and HSP90 (3O0I). Biovia Discovery Studio Client 2025 was used to remove water and heteroatoms. AutoDock Tools 1.5.7 was used to prepare the protein. Polar hydrogen and Kollman charge were added. The prepared proteins were saved in PDBQT format. Grid parameters were calculated using the grid menu available in AutoDock. The default values of centers and coordinates were taken for docking [32, 33].

2.12.2 Ligand Preparation

The ligand structure was downloaded from the PubChem database (https://pubchem.ncbi.nlm.nih.gov/) in 3d sdf format. It was converted into PDB format using PyMOL. AutoDock Tools 1.5.7 was used to prepare the ligand. It was then saved in the PDBQT format for docking.

2.12.3 Visualization

To visualize the receptor-ligand complex, Biovia Discovery Cient 2025 was used.

3. Results

3.1 Effect of etoricoxib on organ wet weight in 2K1C rats

We investigated different organ weights to determine if any noticeable changes occurred between the disease and treatment groups (Figure 1). The heart weight, left ventricular weight, right ventricular weight, liver and spleen weight did not show any significant difference in the disease group compared to the control group. The spleen weight was slightly higher in the disease group. Similarly, the treatment groups did not vary in weight compared to the other groups. However, the weight of the unclipped kidney of the 2K1C disease group

significantly increased in comparison with the control group. The Control + Etoricoxib group showed a significant reduction ($p \leq 0.01$) in kidney weight than the disease group, moreover, it showed an abnormally low kidney weight compared to the controlled group of rats. The 2K1C + Etoricoxib treatment group could not lower the kidney weight significantly compared to the 2K1C disease group (Figure 1D).

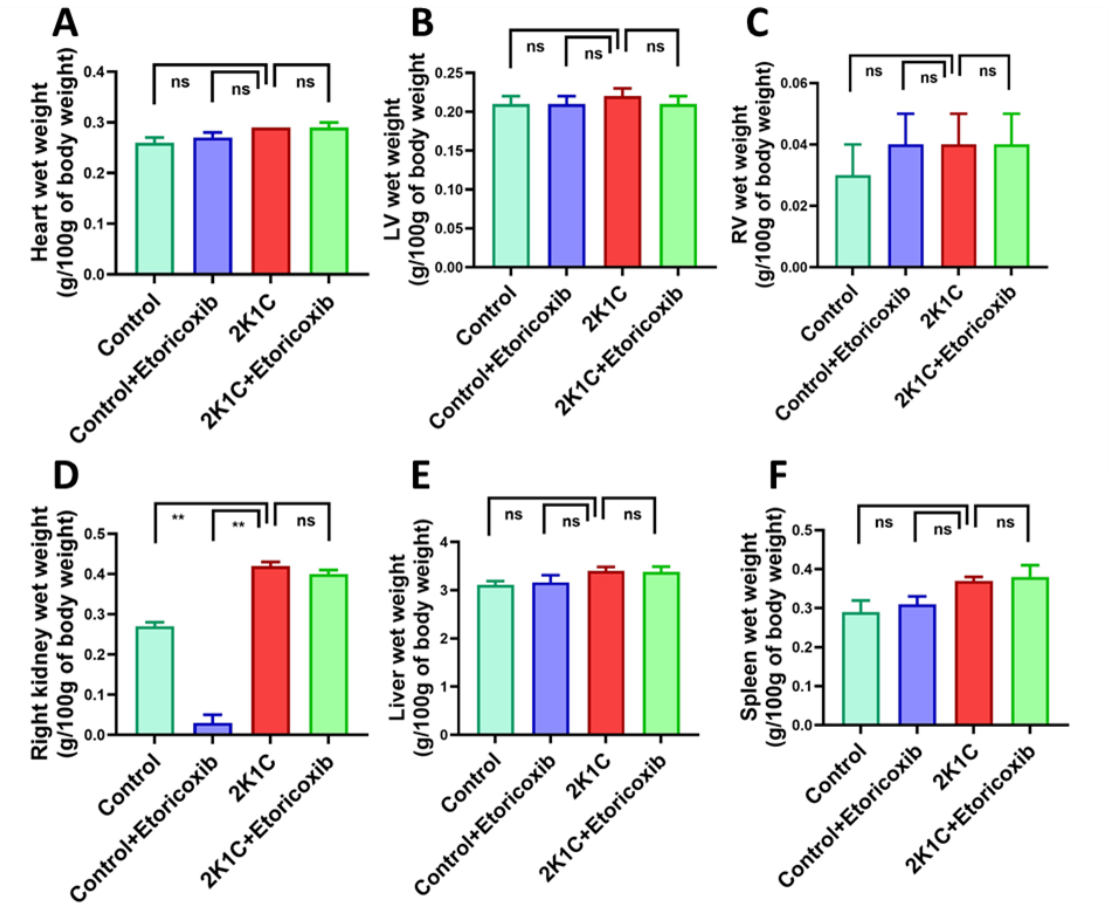

Figure 1: Effect of etoricoxib on (A) the heart, (B) left ventricle, (C) right ventricle, (D) kidney, (E) liver, and (F) spleen wet weight of the 2K1C rat model. N=6 in every group, each bar is presented as mean ± SEM. Statistical analysis was conducted using One-way ANOVA with Tukey's post hoc test, where ** indicates $p \leq 0.01$, * indicates $p \leq 0.05$, and ns indicates $p > 0.05$.

3.2 Effect of etoricoxib on biochemical parameters AST, ALT, and ALP activity

Biochemical measurement showed a significant increase in plasma AST, ALT, and ALP activity in 2K1C rats compared to the control rats (Fig. 2). Treatment with etoricoxib in 2K1C rats significantly neutralized ($p \leq 0.01$) the increased enzyme activity of AST and ALP. The reduction in the ALT activity was not significant enough, but it tended to lower it (Fig. 2B). In addition, the Control + Etoricoxib group showed significantly low ($p \leq 0.01$) and normalized values compared to the disease group in case of all three liver enzyme activities.

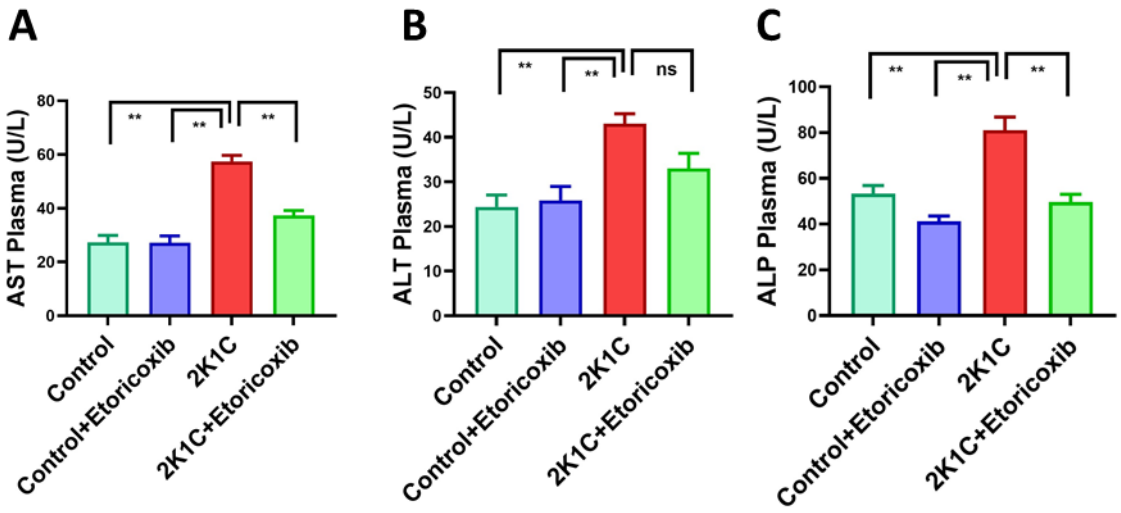

Figure 2: Effect of Etoricoxib on plasma liver enzymes (A) AST, (B) ALT, and (C) ALP levels of the 2K1C rat model. N=6 in every group, each bar is presented as mean ± SEM. Statistical analysis was conducted using One-way ANOVA with Tukey's post hoc test, where ** indicates $p \leq 0.01$, * indicates $p \leq 0.05$, and ns indicates $p > 0.05$.

3.3 Effect of etoricoxib on oxidative stress markers

To determine the oxidative stress in our study, the oxidative stress parameters malondialdehyde (MDA), nitric oxide, and advanced oxidation protein product (AOPP) content in plasma, heart, and kidneys were evaluated.

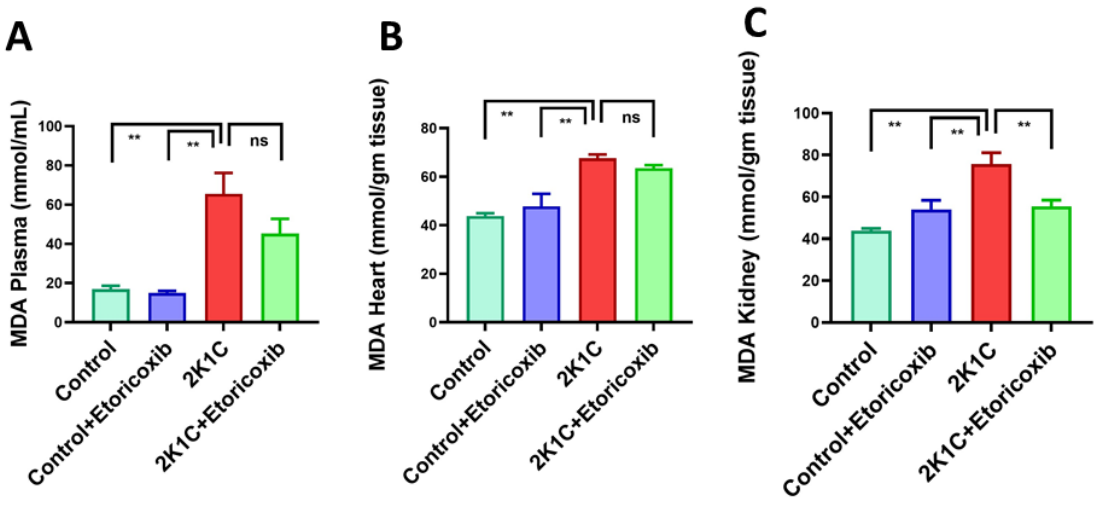

Figure 3: Effect of Etoricoxib on MDA level in (A) plasma, (B) heart, and (C) kidney homogenates of the 2K1C rat model. N=6 in every group, each bar is presented as mean ± SEM. Statistical analysis was conducted using One-way ANOVA with Tukey's post hoc test, where ** indicates $p \leq 0.01$, * indicates $p \leq 0.05$, and ns indicates $p > 0.05$.

A higher concentration of MDA (A lipid peroxidation product) in plasma, heart, and kidney of 2K1C rats was observed (Fig. 3). Etoricoxib treatment in 2K1C rats significantly reduced ($p \leq 0.01$) the level of MDA (lipid peroxides) in the kidney compared to the 2K1C group in plasma, heart, and kidney. However, the treatment also reduced the plasma and heart MDA levels, but not to a significant extent. The Control + Etoricoxib group showed normal levels similar to or closer to the control group.

Nitric oxide (measured as nitrate) was also increased in the hearts and kidneys of the 2K1C group compared to the control rats, which was further reduced by etoricoxib treatment in the 2K1C group (Fig. 4). The NO concentration in the disease group increased by a non-significant amount in the plasma. The kidney NO levels showed a significantly low value ($p \leq 0.01$) compared to the disease group. Although the NO concentration in plasma and heart was reduced by the drug, but not significant enough. In the case of the Control + Etoricoxib group, it showed a significantly lower value in plasma, heart ($p \leq 0.05$), and kidney ($p \leq 0.01$) compared to the 2K1C group.

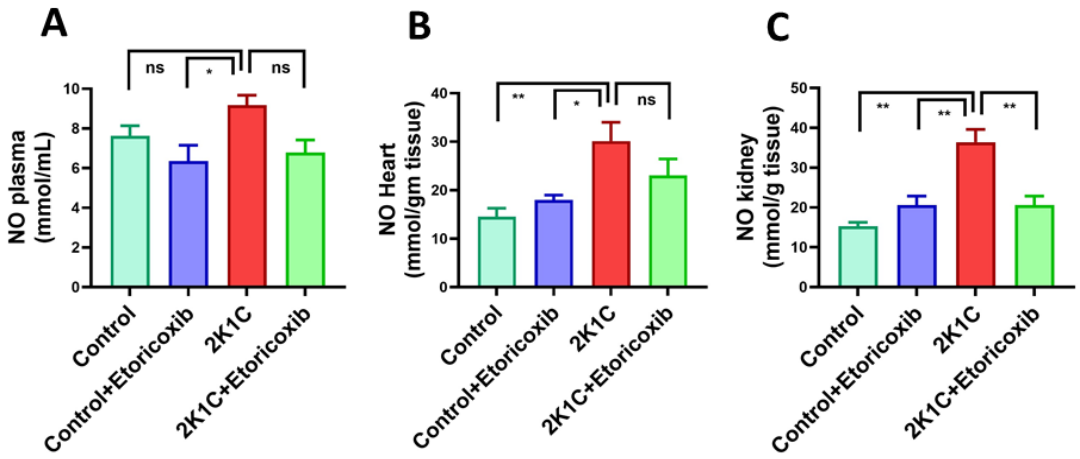

Figure 4: Effect of Etoricoxib on NO level in (A) plasma, (B) heart, and (C) kidney homogenates of the 2K1C rat model. N=6 in every group, each bar is presented as mean ± SEM. Statistical analysis was conducted using One-way ANOVA with Tukey's post hoc test, where ** indicates *p ≤ 0.01*, * indicates *p ≤ 0.05*, and ns indicates *p> 0.05.*

2K1C rats demonstrated a significant increase ($p \leq 0.01$) in the concentration of AOPP in plasma and heart, which was reduced but at a nonsignificant extent when treated with etoricoxib (Fig. 5). The Control + Etoricoxib treatment group showed significantly low ($p \leq 0.01$) AOPP value relative to the disease group.

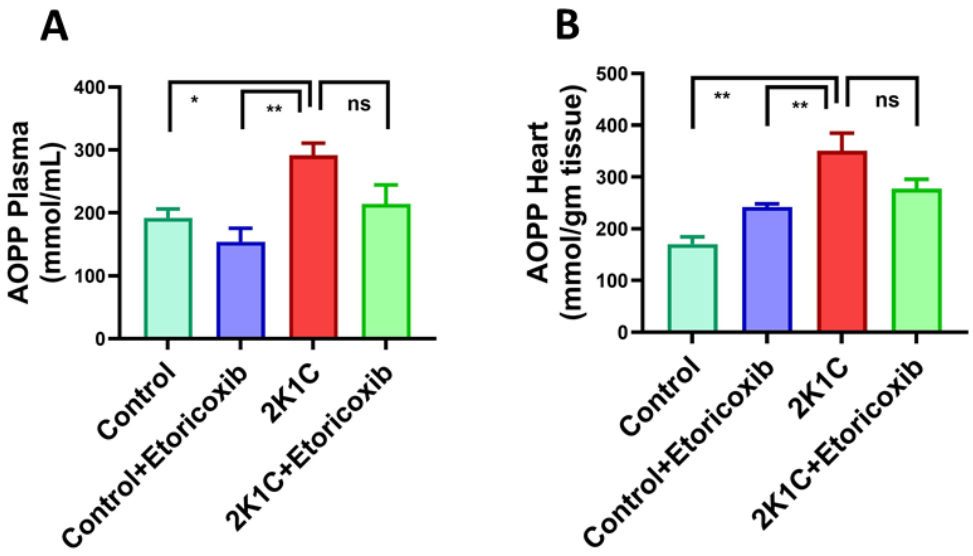

Figure 5: Effect of Etoricoxib on AOPP level in (A) plasma, (B) heart homogenates of 2K1C rat model. N=6 in every group, each bar is presented as mean ± SEM. Statistical analysis was conducted using One-way ANOVA with Tukey's post hoc test, where ** indicates $p \leq 0.01$, * indicates $p \leq 0.05$, and ns indicates $p > 0.05$.

3.4 Effect of etoricoxib on histological parameters

Hematoxylin and Eosin (H&E) and Picric acid-Sirius red staining were done on both heart and kidney sections of different study groups, and microscopic photographs were taken with 40X magnification (Fig. 6 and 7).

In the case of the heart H&E staining, the histopathological images showed distorted tissue structure and a high concentration of inflammatory cell accumulation in the cardiac tissue of the 2K1C disease group (Figure 6C). The 2K1C + Etoricoxib treatment group exhibited comparatively low inflammatory cell counts and better tissue structure than the disease group. The Control + Etoricoxib group showed no inflammatory cell infiltration and normal cellular structure, similar to the control group.

In picrosirius red staining, a high amount of fibrosis in the heart of the 2K1C rat was observed in comparison to the control group. Etoricoxib-treated groups demonstrated notably less fibrosis than the 2K1C group (Fig. 6).

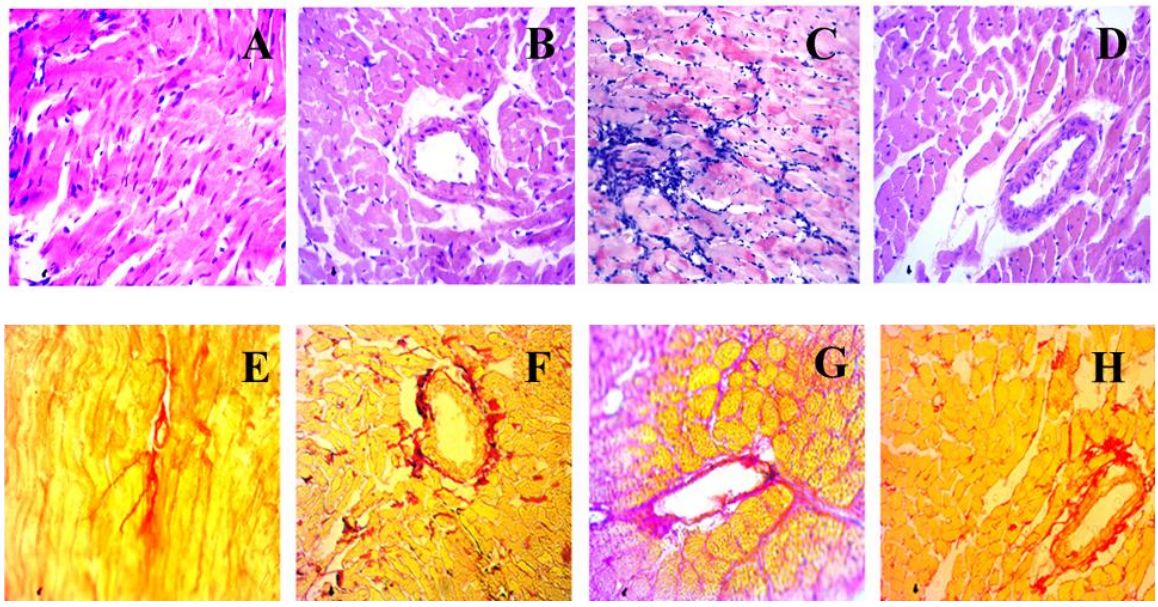

Figure 6: Effect of Etoricoxib on the heart histology of 2K1C rat model at 40x magnification. Upper row- H&E staining where A. Control; B. Control + Etoricoxib; C. 2K1C; D. 2K1C + Etoricoxib. Lower row- Picrosirius red staining where E. Control; F. Control + Etoricoxib; G. 2K1C; H. 2K1C + Etoricoxib.

The kidney tissue of the 2K1C disease group showed a high inflammatory cell accumulation and fibrotic deposition compared to the control group. The etoricoxib treatment tended to reduce the inflammation and ameliorate the fibrosis in the kidney tissue (Fig. 7).

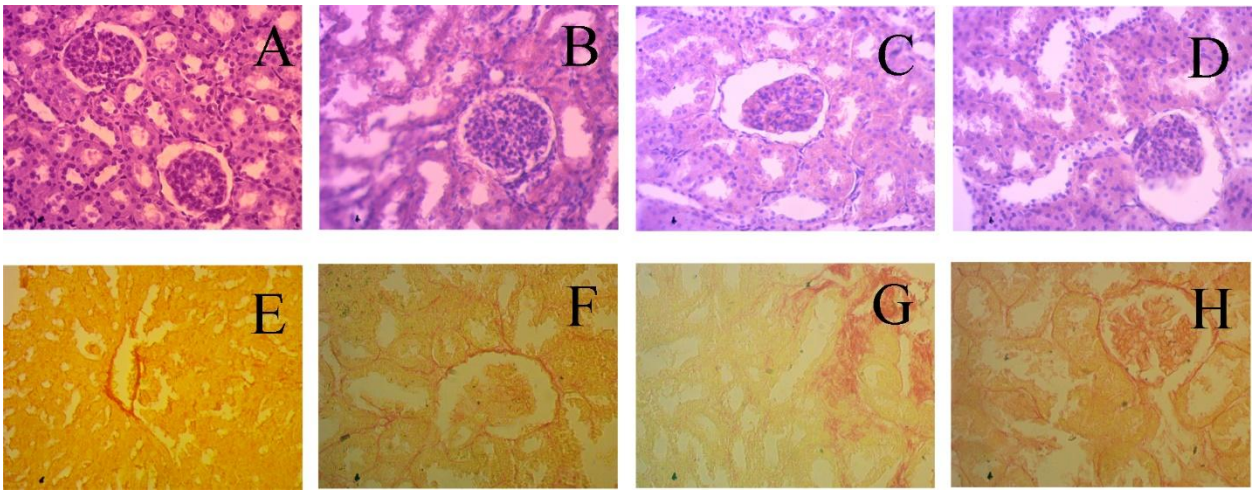

Figure 7: Effect of Etoricoxib on the kidney histology of the 2K1C rat model at 40x magnification. Upper row- H&E staining where A. Control; B. Control + Etoricoxib; C. 2K1C; D. 2K1C + Etoricoxib. Lower row- Picrosirius red staining, where E. Control; F. Control + Etoricoxib; G. 2K1C; H. 2K1C + Etoricoxib.

3.5 Network Pharmacology

3.5.1 Target Interaction Analysis

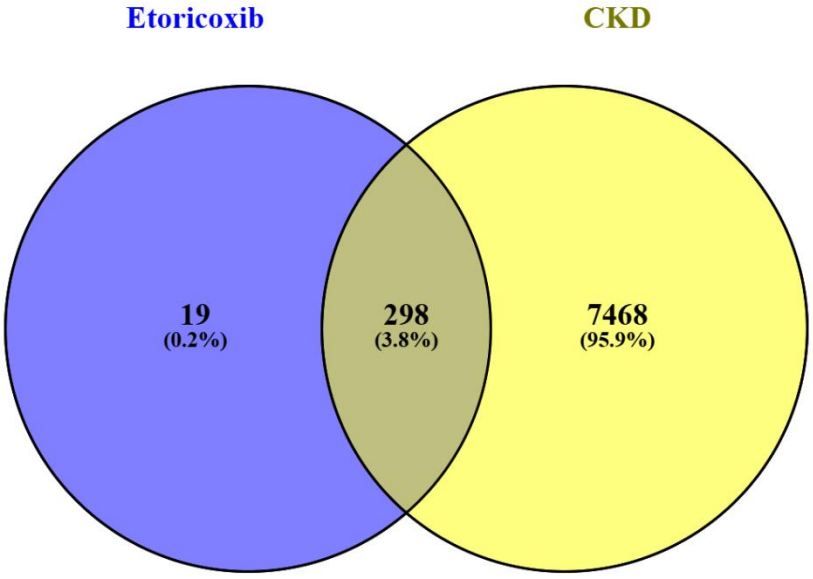

Figure 8: Venn diagram showing the intersection of Etoricoxib targets and chronic kidney disease genes. The overlap identifies 298 core therapeutic targets.

A Venn diagram is used to identify the common factors. Here, common genes of chronic kidney disease and the etoricoxib target gene were identified. Chronic kidney disease-related genes were collected from Genecards Database. A total of 7766 genes were found responsible for the development of the disease. The intersected portion of the diagram showed 298 genes targeted by etoricoxib.

3.5.2 PPI Construction

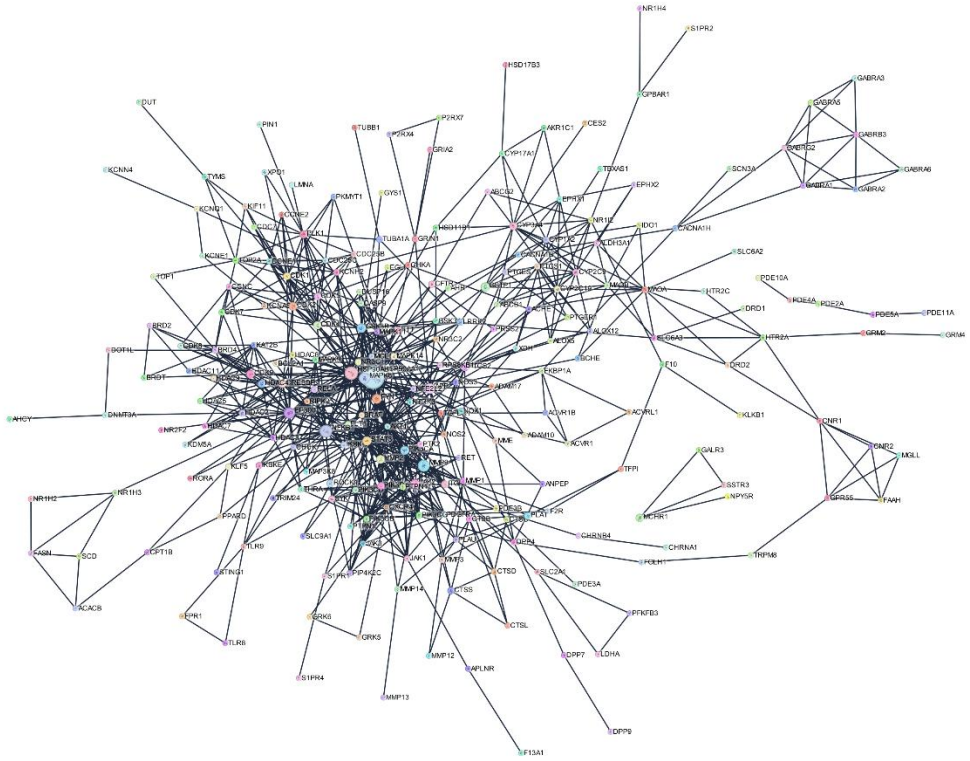

Figure 9: Protein-Protein Interaction (PPI) network of the 298 intersecting targets. Core hub genes are positioned centrally. Node size and color gradients map to connectivity and topological importance.

298 overlapping genes formed a dense network. It indicates they are strongly connected to each other. Cytoscape analyzed topological parameters that highlighted the core nodes that mediate the pathway. Nodes with a larger size and stronger color represent genes with higher importance and connectivity. These central proteins act like communication hubs within the

network. AKT1, HSP90AA1, EP300, CREBBP, FYN, and APP showed the highest degree, which are 43, 24, 24, 20, 17, and 17, respectively. It indicates that etoricoxib mediates cell proliferation, apoptosis, and vascular calcification.

3.5.3 Merged Network Analysis

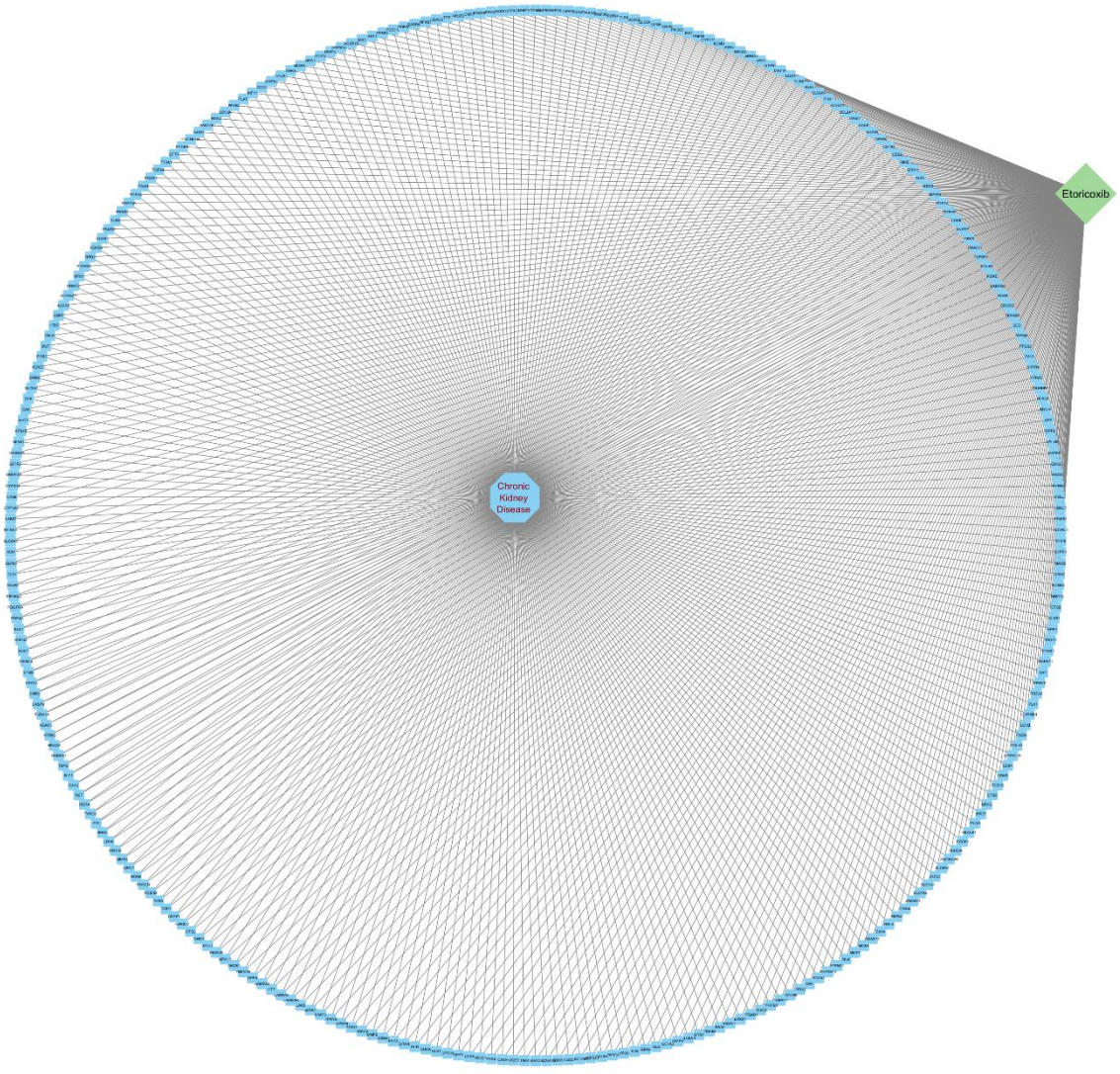

Figure 10: Merged Compound-Target-Disease network. The constructed map demonstrates the direct multi-target relationships between etoricoxib and key genes associated with chronic kidney disease.

Figure 10 describes the merged network of the 298 common genes targeted by etoricoxib. The blue octagon-shaped structure reflects the chronic kidney disease. Etoricoxib is highlighted in a green colored diamond. The common genes are reflected in a blue rectangle.

3.5.4 Go Functional Enrichment

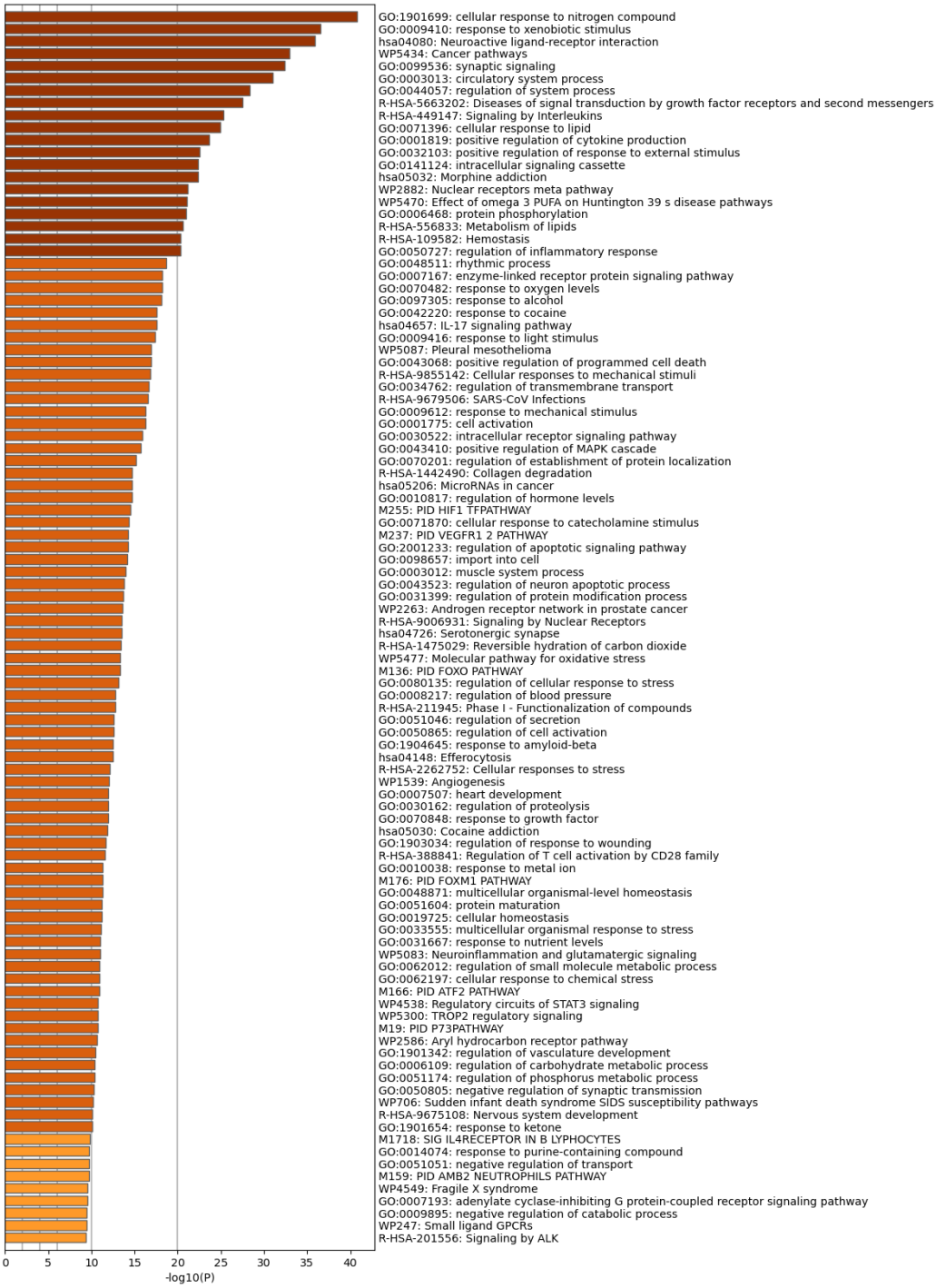

Figure 11: Heatmap detailing the top Gene Ontology (GO) enriched biological processes for the 298 intersecting targets.

Gene Ontology (GO) enrichment analysis explains the specific biological roles of a target gene set. The targeted 298 genes play multiple biological roles. The color of the bar graph indicates the gene's involvement in the processes. Darker colors indicate stronger statistical significance and lower adjusted p-values. The top enriched biological processes were primarily associated with circulatory regulation, inflammatory response, lipid metabolism, and interleukin signaling, which are significant in our animal model study.

3.5.5 PI3/AKT signaling pathway

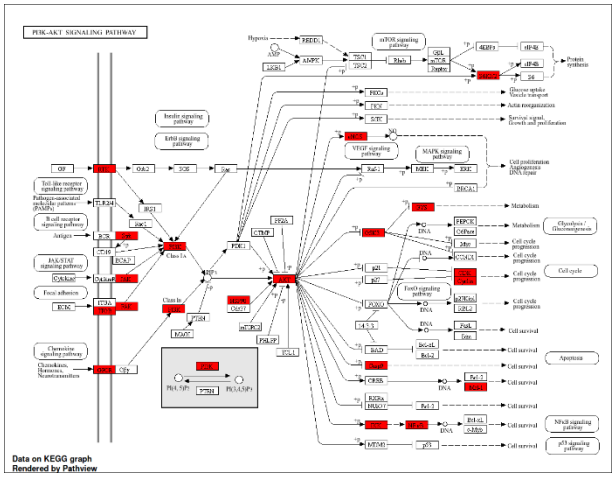

Figure 12: KEGG map of the PI3/AKT signaling pathway. Red highlights represent the genes involved in disease progression and the target of Etoricoxib.

The PI3/AKT signaling pathway is involved in cell cycle, cell survival, inflammation, metabolism, and apoptosis. The red-highlighted genes are the target of etoricoxib. Etoricoxib modulates the signaling pathway by reacting with these genes.

3.6 Molecular Docking Visualization

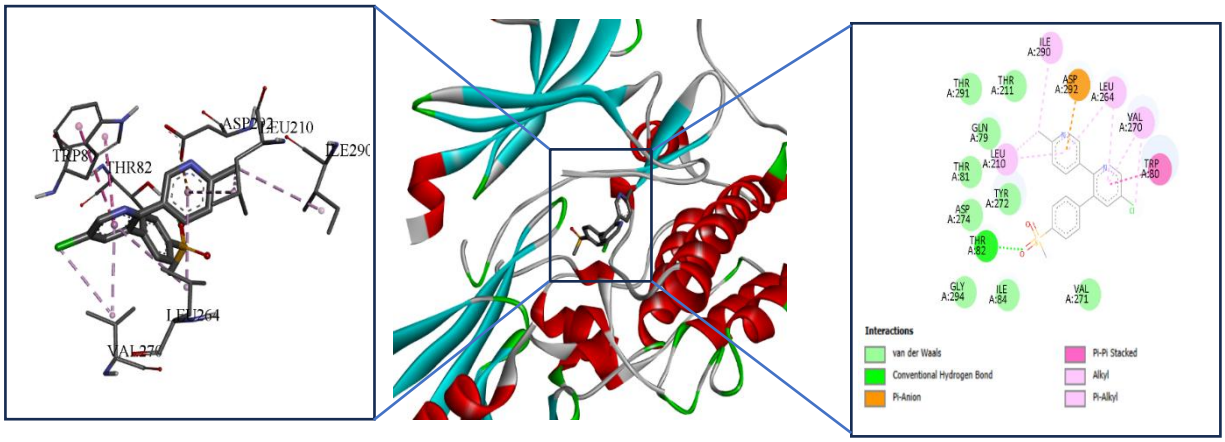

(a)

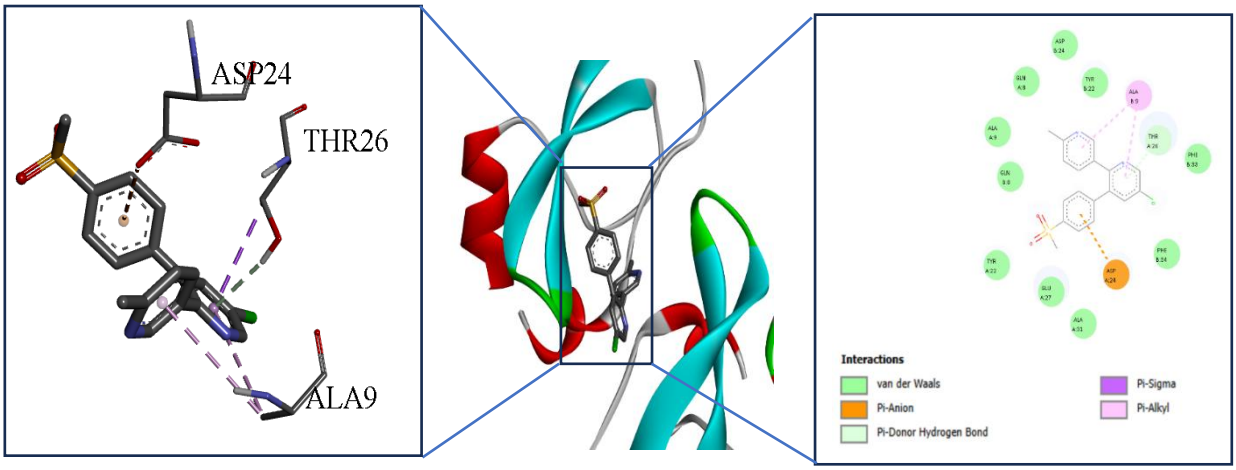

(b)

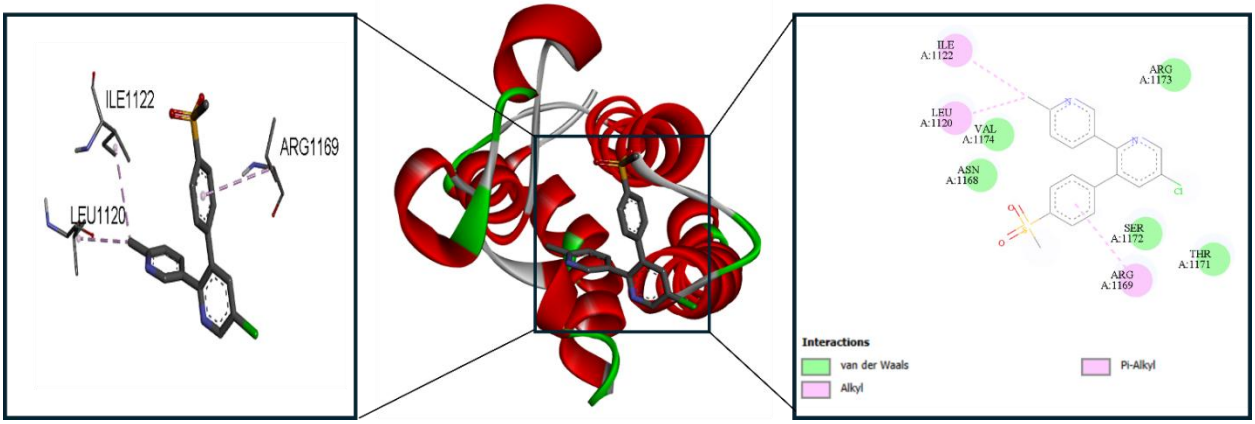

(c)

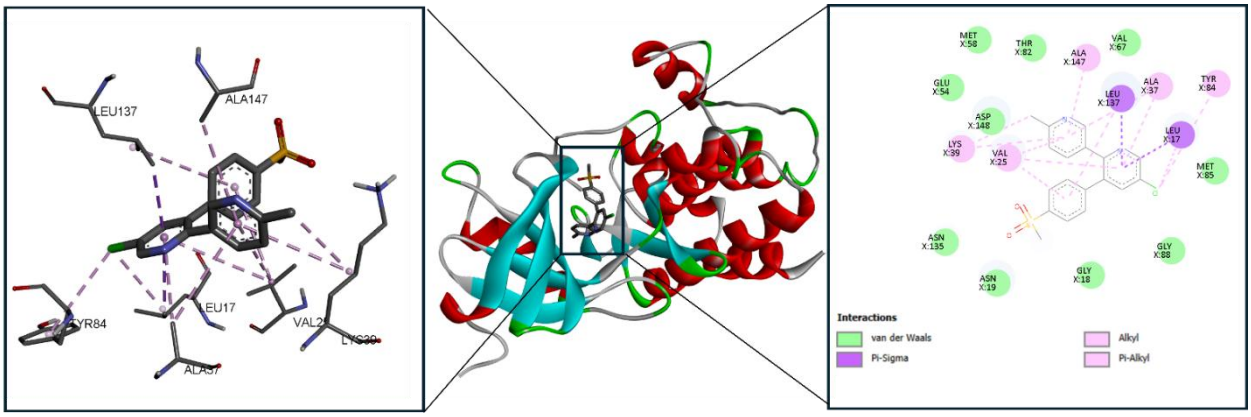

(d)

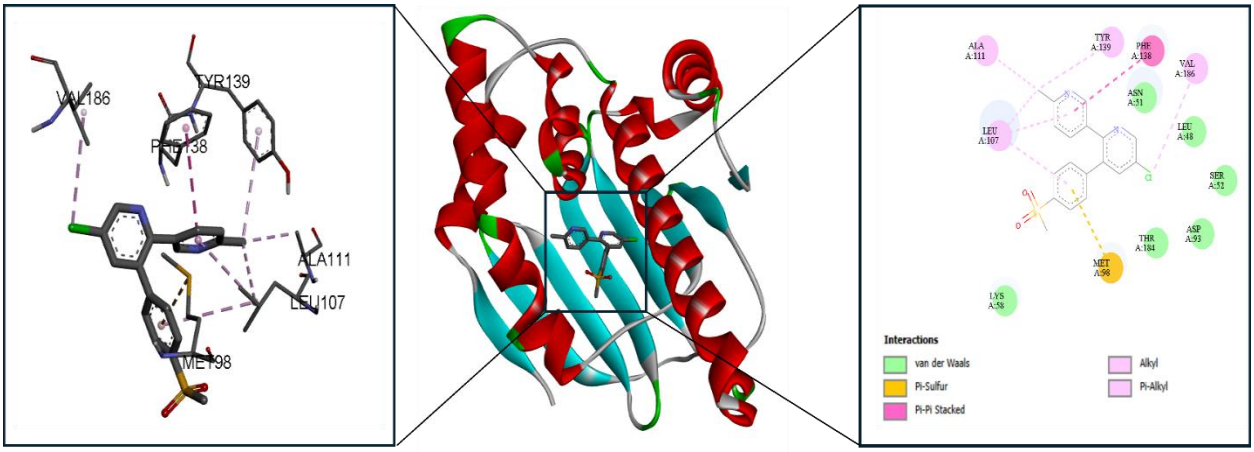

(e)

Figure 13: Visualization of receptor-ligand interaction. (a) Etoricoxib and AKT (4EJN), (b)Etoricoxib and APP (1AAP), (c) Etoricoxib and CREBP (4TQN), (d) Etoricoxib and FYN (2DQ7), (e) Etoricoxib and HSP90 (3O0I)

Table 1: Molecular Docking interaction of Etoricoxib with AKT (4EJN), APP (1AAP), CREBP (4TQN), FYN (2DQ7), HSP90 (3O0I)

Protein	Ligand	Binding Affinity (Kcal/mol)	Bond Type	Amino Acid residue	Bond Length
AKT1	Etoricoxib	-9.6	Conventional Hydrogen Bond	THR A:82	2.11
			Pi-Anion	ASP A:292	4.65
			Pi-Pi Stacked	TRP A:80	4.68
			Alkyl	LEU A:210	4.63
				ILE A:290	4.92
				VAL A:270	4.28
			Pi-Alkyl	LEU A:210	4.87
				LEU A:264	5.19
				LEU A:264	5.41
				VAL A:270	4.28
APP	Etoricoxib	-6.2	Pi Donor Hydrogen Bond	THR A:26	2.72
			Pi-Anion	ASP A:24	4.20
			Pi-Alkyl	ALA A:9	4.81
				ALA A:9	4.96
			Pi-Sigma	THR A:26	3.74
CREBP	Etoricoxib	-6.6	Alkyl	ILE A:1122	4.00
				LEU A:1120	4.18
			Pi-Alkyl	ARG A:1169	4.90
FYN	Etoricoxib	-8.4	Alkyl	LYS X:39	3.97
				LEU X:17	3.97
			Pi-Alkyl	LYS X:39	5.14
				VAL X:25	4.69
				VAL X:25	4.82

				VAL X:25	5.41
				ALA X:37	4.42
				ALA X:37	5.07
				ALA X:147	4.69
				LEU X:137	5.40
				TYR X:84	4.99
			Pi-Sigma	LEU X:17	3.97
				LEU X:137	3.61
HSP	Etoricoxib	-7.9	Alkyl	ALA A:111	3.96
				LEU A:107	4.59
				VAL A:186	4.88
			Pi-Alkyl	LEU A:107	4.54
				LEU A:107	4.97
				TYR A:139	5.13
			Pi-Sulfur	MET A:98	4.75
			Pi-Pi Stacked	PHE A:138	5.06

Discussion

This study demonstrated that etoricoxib treatment prevented oxidative stress, inflammatory cell infiltration, and fibrosis in the hearts and kidneys of 2-kidney one-clip (2K1C) rats. Kidney impairment due to stenosis, atherosclerosis, or excessive oxidative stress and further development or progression into other significant diseases like hypertension, cardiovascular disease, chronic kidney disease, diabetes, etc., has become more and more common without any permanent cure [34, 35]. This study demonstrated the effect of one of the COX-2 inhibitors, etoricoxib, on improving the kidney impairment and related conditions in the 2K1C rat model. There is a common and direct proportional relation between ROS, the RAS system, and the COX-2 enzyme. Each one is interconnected with the others [36-38]. Previous studies revealed that 2K1C rats have an overactivated Angiotensin II pathway, which further develops hypertension and endothelial impairment due to increased free radical-mediated oxidative stress [39]. Also, the elevation of systolic blood pressure due to hypertension causes oxidative

stress, which causes overexpression of COX-2. COX-2 has an important role in developing renovascular hypertension in our 2K1C rat [40].

Our investigation on organ wet weights demonstrates that there were no noticeable changes between the disease group and the other groups. The whole heart, LV, RV, liver, and spleen showed a slight increase in the weights in the disease group, but it was nonsignificant. The treatment with etoricoxib did not affect weight reduction in case of any of these organs, and even the right unclipped kidney. However, the 2K1C disease group showed a significant increase in the case of the right kidney weight compared to the control group. This might be due to the hyperperfusion and where this one kidney had to take all the load of blood flow and the filtration process, as the other kidney was clipped [41].

Oxidative stress parameters like MDA, NO, and AOPP revealed how much the 2K1C disease group caused protein degradation, lipid peroxidation, and further production of ROS, and to what extent it caused other organ damage. MDA, or malondialdehyde, is the indicator of lipid peroxidation and can be measured to monitor oxidative stress [42]. Polyunsaturated fatty acids (PUFA) in membranes are attacked by hydroxyl radicals created by elevated H_2O_2. This results in a reactive carbon radical that combines with oxygen to form peroxyl radicals. Lipid peroxides are produced by this peroxyl radical in a self-amplifying manner, causing extensive damage and, ultimately, membrane breakdown [43]. Our study illustrated a significantly high MDA concentration in the plasma, heart, and kidney. Etoricoxib treatment reduced MDA levels, but it was significant only for the kidney. The control and control + etoricoxib group showed a similar level in case of MDA concentration, indicating etoricoxib did not cause any unwanted lipid peroxidation (Fig. 3).

Another biomarker of oxidative stress is excess nitric oxide (NO), which in the normal range is crucial for different physiological processes like immune response, blood vessel dilation, neurotransmission, etc. [44]. NO is a free radical, and when it reacts with O^{-2-} (superoxide anion), it produces a nitrosating agent and potent oxidant $ONOO^-$ (peroxynitrite), which can damage tissues and cells and give rise to various diseases [45]. In our study, the NO

concentration showed a significantly high level in the heart and kidney; the plasma NO concentration was also high, but was not significant enough. Our etoricoxib treatment reduced all NO concentrations in plasma, heart, and kidney, but only the reduction of kidney NO concentration was significant. In all cases, the control and control+ etoricoxib groups showed almost similar NO concentration (Fig. 4).

ROS reacts with proteins, causing damage and producing a modified form of protein called AOPP or advanced oxidation protein products, another oxidative stress index [46]. In the study, the 2K1C disease group showed a significantly higher amount of AOPP in plasma and heart compared to both of the control groups. The etoricoxib treatment tended to reduce the AOPP level, but it was not significant enough (Fig. 5).

AST, ALT, and ALP are liver enzymes usually used for determining liver health. Their function is to metabolize amino acids in various tissues, including the heart, muscle, and liver, so high levels of these enzymes might indicate heart damage [47, 48]. Heart failure and renal dysfunction can elevate the levels of AST, ALT, and ALP, as heart failure can lead to hepatic hypoxia, and metabolic dysfunction can occur due to renal disease [49]. This study displayed a significant elevation in all three enzymes in the 2K1C disease group in comparison with the control groups. Our treatment with etoricoxib successfully reduced all three enzymes, especially AST and ALP, at a significant level. The control + etoricoxib group showed a similar level of these enzymes compared to the control group (Fig. 2).

Hyperperfusion and the overload to one kidney, and additional generation of oxidative stress, can damage the healthy kidney [50]. The filtering unit of the kidney glomerulus can be destroyed, and glomerulonephritis can occur, which is an inflammatory condition of the glomeruli [51, 52]. This might lead to further progression of kidney disease and other diseases which are directly or indirectly linked to the kidney through blood and other cellular signaling cascades, especially the heart [53, 54]. In this investigation, the histopathological study of the heart and kidney was done to find out the cellular condition of both these organs. Hematoxylin and Eosin and Picrosirius red staining were performed.

In the heart histology, the H&E staining demonstrated the destroyed cardiomyocytes and excessive inflammatory cell accumulation in the 2K1C disease group. We can also observe the control and control + etoricoxib group (Fig.6A, 6B) with normal cellular structure, where no inflammation occurred. The disease group treated with etoricoxib showed much fewer inflammatory cells and an intact myocardial structure. This indicates that etoricoxib successfully reduces the inflammation and protects the heart from the disease.

Also, the Sirius red staining in the disease group showed fibrotic and collagen deposition, which usually occurs as scar tissue after an occurrence of damage. The collagen and fibrotic deposition are much less in the etoricoxib treatment + 2K1c disease group, which indicates that the treatment ameliorated the damage (Fig. 6H). The control and control+ etoricoxib group is showing normal condition in this staining.

Similarly, the kidney histology of the right kidney showed inflammatory cells, and a reduced size of the glomerulus in the H&E staining (Fig. 7C). Etoricoxib treatment could not properly protect the kidney but tended to reduce the inflammation (Fig. 7D). The Sirius red staining showed collagen deposition in the kidney (Fig. 7G), which was normalized by the etoricoxib treatment (Fig. 7H).

Molecular docking analysis was performed to evaluate the binding interactions of etoricoxib with the key central proteins identified in the network pharmacology analysis: AKT1, APP, CREBP, FYN, and HSP. The docking results demonstrated favorable binding affinities for all selected targets, indicating the potential of etoricoxib to interact with multiple proteins involved in disease-associated molecular pathways.

Among all targets, etoricoxib exhibited the strongest binding affinity toward AKT1, with a docking score of −9.6 kcal/mol, suggesting a highly stable ligand–protein complex. This is due to the formation of a conventional hydrogen bond with THR82 at a bond distance of 2.11 Å, which likely contributes significantly to complex stabilization. Additionally, π-anion interaction with ASP292, π–π stacking with TRP80, and multiple alkyl and π-alkyl interactions involving residues LEU210, ILE290, VAL270, and LEU264 further strengthened binding

within the active site. The presence of multiple hydrophobic and electrostatic interactions indicates a strong complementarity between etoricoxib and the AKT1 binding site.

Etoricoxib also demonstrated stable binding with FYN, exhibiting a docking score of −8.4 kcal/mol. The interaction showed mainly hydrophobic contacts, including multiple alkyl and π-alkyl interactions with residues such as LYS39, LEU17, VAL25, ALA37, ALA147, LEU137, and TYR84. Furthermore, π-sigma interactions with LEU17 and LEU137 suggest additional stabilization of the ligand within the binding pocket. These non-covalent interactions may explain the relatively strong binding observed for this target.

HSP also showed favorable binding with etoricoxib, with a binding energy of −7.9 kcal/mol. The ligand formed several alkyl and π-alkyl interactions involving ALA111, LEU107, VAL186, and TYR139, along with π-sulfur interaction with MET98 and π–π stacked interaction with PHE138. Such interactions suggest that etoricoxib fits well within the hydrophobic region of the HSP binding pocket.

Moderate binding affinities were observed for CREBP (−6.6 kcal/mol) and APP (−6.2 kcal/mol). In CREBP, etoricoxib formed alkyl interactions with ILE1122 and LEU1120, as well as π-alkyl interaction with ARG1169, indicating hydrophobic stabilization. In APP, the ligand formed a π-donor hydrogen bond with THR26, π-anion interaction with ASP24, π-alkyl interactions with ALA9, and π-sigma interaction with THR26. Although the binding energies for these proteins were comparatively lower, the presence of multiple stabilizing interactions may be responsible for modulating disease.

Pathway enrichment analysis revealed that the identified hub targets were significantly enriched in the PI3K–AKT signaling pathway, suggesting that this signaling cascade may represent a major mechanistic route underlying the therapeutic activity of etoricoxib. Mapping the core targets onto the KEGG PI3K–AKT pathway revealed the involvement of multiple key regulatory proteins, indicating their influence on upstream receptor-mediated signaling and downstream transcriptional responses.

The PI3K–AKT pathway regulates diverse cellular processes, including cell survival, proliferation, metabolism, apoptosis, and inflammatory responses [55]. In the present analysis, AKT1 acts as a central signaling node (Figure 12), consistent with molecular docking results showing that etoricoxib exhibited the strongest binding affinity for AKT1 (−9.6 kcal/mol). This strong interaction suggests that etoricoxib may directly influence AKT-mediated phosphorylation, potentially modulating downstream effectors involved in cell survival and anti-apoptotic signaling.

Conclusion

This study concluded that etoricoxib, a COX-2 inhibitor, effectively reduced oxidative stress, particularly lipid peroxidation, normalized liver enzymes, and protected the kidney and heart from fibrotic deposition and inflammation. Further research is required to establish the clinical benefit of etoricoxib in inflammation and fibrosis in atherosclerotic and kidney patients.

Author Contributions: Conceptualization, MAA and NS; methodology, MAA, NS, SS; formal analysis, RB, MTH, OZ; investigation, SS, MHS, MUS; resources, RB, SA, OZ; data curation, SS, SA, MTH; writing—original draft preparation, SS, MTH, SA, OZ; writing—review and editing, MHS, RB, MUS; visualization, MAA, NS; supervision, MAA, NS; project administration, NS; All authors have read and agreed to the published version of the manuscript.

Funding: This research received no external funding.

Institutional Review Board Statement: The Institutional Animal Care and Use Committee (IACUC) approved the experimental protocol; the approval number is 2025/OR-NSU/IACUC/0702.

Data Availability Statement: Data used in this study will be available upon reasonable request from the corresponding author.

Acknowledgments: The authors cordially acknowledge the logistic support and laboratories facilities from the Department of Pharmaceutical Sciences, North South University.

Conflicts of Interest: The authors declare no conflict of interest.

References:

1. Bikbov, B., et al., *Global, regional, and national burden of chronic kidney disease, 1990–2017: a systematic analysis for the Global Burden of Disease Study 2017.* The lancet, 2020. **395**(10225): p. 709-733. https://doi.org/10.1016/S0140-6736(20)30045-3
2. Chen, J.; Deng, M.; Zheng, R.; Chen, Y.; Pang, W.; Zhang, Z.; Tan, Z.; Bai, Z. Global, regional, and national trends in chronic kidney disease burden (1990–2021): a systematic analysis of the global burden of disease in 2021. *Trop. Med. Health* **2025**, *53(1)*, 26. https://doi.org/10.1186/s41182-025-00703-x
3. Parsegian, K.; Trivedi, R.; Ioannidou, E. Renal Diseases. *Burket's Oral Med.* **2021**, 579-626. https://doi.org/10.1002/9781119597797.ch16
4. Kalantar-Zadeh, K.; Jafar, T. H.; Nitsch, D.; Neuen, B. L.; Perkovic, V. Chronic kidney disease. *Lancet* **2021**, *398(10302)*, 786-802. https://doi.org/10.1016/S0140-6736(21)00519-5
5. Vargas, R. A. V.; Millán, J. M. V.; Bonilla, E. F. Renin–angiotensin system: Basic and clinical aspects—A general perspective. *Endocrinol. Diabetes Nutr.* **2022**, *69(1)*, 52-62. https://doi.org/10.1016/j.endien.2022.01.005
6. Su, C.; Xue, J.; Ye, C.; Chen, A. Role o f the central renin-angiotensin system in hypertension. *Int. J. Mol. Med.* **2021**, *47(6)*, 95. https://doi.org/10.3892/ijmm.2021.4928
7. Zamani-Garmsiri, F.; Emamgholipour, S.; Rahmani Fard, S.; Ghasempour, G.; Jahangard Ahvazi, R.; Meshkani, R. Polyphenols: potential anti-inflammatory agents for treatment of metabolic disorders. *Phytother. Res.* **2022**, *36(1)*, 415-432 https://doi.org/10.1002/ptr.7329
8. Avila-Carrasco, L.; Majano, P.; Sánchez-Toméro, J. A.; Selgas, R.; López-Cabrera, M.; Aguilera, A.; González Mateo, G. Potential therapeutic effects of natural plant compounds in kidney disease. *Molecules* **2021**, *26(20)*, 6096. https://doi.org/10.3390/molecules26206096
9. Bhullar, S. K.; Dhalla, N. S. Angiotensin II-induced signal transduction mechanisms for cardiac hypertrophy. *Cells* **2022**, *11(21)*, 3336. https://doi.org/10.3390/cells11213336
10. Rotariu, D.; Babes, E. E.; Tit, D. M.; Moisi, M.; Bustea, C.; Stoicescu, M.; Radu, A. F.; Vesa, C. M.; Behl, T.; Bungau, A. F.; et al. Oxidative stress–Complex pathological issues concerning the hallmark of cardiovascular and metabolic disorders. *Biomed. Pharmacother.* **2022**, *152*, 113238. https://doi.org/10.1016/j.biopha.2022.113238
11. Faki, Y.; Er, A. Different chemical structures and physiological/pathological roles of cyclooxygenases. *Rambam Maimonides Med. J.* **2021**, *12(1)*, e0003. https://doi.org/10.5041/RMMJ.10426
12. Xu, C.; Fang, H.; Zhou, L.; Lu, A.; Yang, T. Na+-retaining action of COX-2 (Cyclooxygenase-2)/EP1 pathway in the collecting duct via activation of intrarenal renin-angiotensin-aldosterone system and epithelial sodium channel. *Hypertension* **2022**, *79(6)*, 1190-1202. https://doi.org/10.1161/HYPERTENSIONAHA.121.17245
13. Savedchuk, S.; Phachu, D.; Shankar, M.; Sparks, M. A.; Harrison-Bernard, L. M. Targeting glomerular hemodynamics for kidney protection. *Adv. Kidney Dis. Health* **2023**, *30(2)*, 71-84. https://doi.org/10.1053/j.akdh.2022.12.003
14. Jaimes, E. A.; Tian, R. X.; Pearse, D.; Raij, L. Up-regulation of glomerular COX-2 by angiotensin II: Role of reactive oxygen species. *Kidney Int.* **2005**, *68(5)*, 2143-2153. https://doi.org/10.1111/j.1523-1755.2005.00670.x
15. Quadri, S. S.; Majid, D. S. Interaction of the renin angiotensin and cox systems in the kidney. *Front. Biosci. (Schol Ed)* **2016**, *8(2)*, 215-226. https://doi.org/10.2741/s459
16. Zhao, Y.; Liu, Y.; Wang, J.; Ma, X.; Yang, J.; Zhang, L.; Zhang, X.; Yin, J. COX-2 is required to mediate crosstalk of ROS-dependent activation of MAPK/NF-κB signaling with pro-inflammatory response and defense-related NO enhancement during

challenge of macrophage-like cell line with *Giardia duodenalis*. *PLoS Negl. Trop. Dis.* **2022**, *16(4)*, e0010402. https://doi.org/10.1371/journal.pntd.0010402

17. Aranda-Rivera, A. K.; Cruz-Gregorio, A.; Pedraza-Chaverri, J.; Scholze, A. Nrf2 activation in chronic kidney disease: promises and pitfalls. *Antioxidants* **2022**, *11(6)*, 1112. https://doi.org/10.3390/antiox11061112
18. Kuczeriszka, M.; Wąsowicz, K. Animal models of hypertension: The status of nitric oxide and oxidative stress and the role of the renal medulla. *Nitric Oxide* **2022**, *125*, 40-46. https://doi.org/10.1016/j.niox.2022.06.003
19. Shuvo, A. U. H.; Alimullah, M.; Jahan, I.; Mitu. K. F.; Rahman, M. J.; Akramaddaula, k.; Khan, F.; Dash, P. R.; Subhan, N.; Alam, M. A. Evaluation of Xanthine Oxidase Inhibitors Febuxostat and Allopurinol on Kidney Dysfunction and Histological Damage in Two-Kidney, One-Clip (2K1C) Rats. *Scientifica* **2025**, *2025(1)*, 7932075. https://doi.org/10.1155/sci5/7932075
20. Gupta, K.; Bagang, K.; Simgh, G.; Arora, S.; Bedi, O.; Kumar, M. Pharmacology of angiotensin in renovascular diseases. In *Angiotensin*, Elsevier: **2023**; pp 151-178. https://doi.org/10.1016/B978-0-323-99618-1.00012-X
21. Okolonkwo, B. B.; Ajibo, D. N.; George-Opuda, I. M.; Donatus, N. J. Recent Trends in Risk Factors Associated with Kidney Diseases. *Asian J. Res. Nephrol.* **2024**, *7(1)*, 7-30.
22. Wu, R.; Lamontagne, D.; de Champlain, J. *Antioxidative properties of acetylsalicylic Acid on vascular tissues from normotensive and spontaneously hypertensive rats.* Circulation, 2002. **105**(3): p. 387-92. https://doi.org/10.1161/hc0302.102609
23. Wu, R.; Laplante, M. A.; De Champlain, J. Prevention of angiotensin II-induced hypertension, cardiovascular hypertrophy and oxidative stress by acetylsalicylic acid in rats. *J. Hypertens.* **2004**, *22(4)*, 793-801. https://doi.org/10.1097/00004872-200404000-00023
24. Suleyman, B.; Albayrak, A.; Kurt, N.; Demirci, E.; Gundogdu, C.; Aksoy, M. The effect of etoricoxib on kidney ischemia-reperfusion injury in rats: a biochemical and immunohistochemical assessment. *Int. Immunopharmacol.* **2014**, *23(1)*, 179-185.https://doi.org/10.1016/j.intimp.2014.06.042
25. Yapca, O. E.; Turan, M. I.; Yilmaz, I.; Salman, S.; Gulapoglu, M.; Suleyman, H. Benefits of the antioxidant and anti-inflammatory activity of etoricoxib in the prevention of ovarian ischemia/reperfusion injury induced experimentally in rats. *J. Obstet. Gynaecol. Res.* **2014**, *40(6)*, 1674-1679.https://doi.org/10.1111/jog.12373
26. Sultana, S.; Eva, S. A.; Siddiqa, S.; Ghosh, H. C.; Amin, M.S.; Rahman, S; Hossen M.T; Subhan, N.; Alam, M. A. Islam M. N. Black seed (Nigella sativa) powder supplementation prevented oxidative stress and cardiac fibrosis in isoprenaline administered rats. J. Bio. Exp. Pharmacol. 2024, 2(1), 31- 45. https://doi.org/10.62624/JBEP00.00 09
27. Tracey, W. R.; Tse, J.; Carter, G. Lipopolysaccharide-induced changes in plasma nitrite and nitrate concentrations in rats and mice: pharmacological evaluation of nitric oxide synthase inhibitors. *J. Pharmacol. Exp. Ther.* **1995**, *272(3)*, 1011-1015. https://doi.org/10.1016/S0022-3565(25)24521-9
28. Jahan, I.; Shuvo, A. U. H.; Alimullah, M.; Rahman, A. S. M. N.; Siddiqua, S.; Rafia, S.; Khan, F.; Ahmed, K. S.; Hossain, H.; Akramaddaula, K.; Alam, M. A.; Subhan, N. Purple potato extract modulates fat metabolizing genes expression, prevents oxidative stress, hepatic steatosis, and attenuates high-fat diet-induced obesity in male rats. *PLoS One* **2025**, *20(4)*, e0318162.https://doi.org/10.1371/journal.pone.0318162
29. Witko-Sarsat, V.; Friedlander, M.; Capeillère-Blandin, C.; Nguyen-Khoa, T.; Nguyen, A. T.; Zingraff, J.; Jungers, P.; Descamps-Latscha, B. Advanced oxidation protein products as a novel marker of oxidative stress in uremia. *Kidney Int.* **1996**, *49(5)*, 1304-1313.https://doi.org/10.1038/ki.1996.186
30. Tiwari, B. K.; Kumar, D.; Abidi, A. B.; Rizvi, S. I. Efficacy of Composite Extract from Leaves and Fruits of Medicinal Plants Used in Traditional Diabetic Therapy against Oxidative Stress in Alloxan-Induced Diabetic Rats. *ISRN Pharmacol.* **2014**, *2014*, 608590. https://doi.org/10.1155/2014/608590

31. Alimullah, M.; Rahman, N.; Sornaker, P.; Akramuddaula, K.; Sarif, S.; Siddiqua, S.; Mitu, K. F.; Jahan, I.; Khan, F.; Subhan, N.; Alam, A. Evaluation of Terminalia arjuna Bark Powder Supplementation on Isoprenaline-Induced Oxidative Stress and Inflammation in the Heart of Long Evans Rats, Understanding the Molecular Mechanism of This Old Medicinal Plant. *J. Med. Nat. Prod.* **2024**, *100004*, 100004–100004. https://doi.org/10.53941/jmnp.2024.100004
32. Forli, S.; Huey, R.; Pique, M. E.; Sanner, M. F.; Goodsell, D. S.; Olson, A. J. Computational Protein–Ligand Docking and Virtual Drug Screening with the AutoDock Suite. *Nat. Protoc.* **2016**, *11(5)*, 905–919. https://doi.org/10.1038/nprot.2016.051
33. Trott, O.; Olson, A. J. AutoDock Vina: Improving the Speed and Accuracy of Docking with a New Scoring Function, Efficient Optimization, and Multithreading. *J. Comput. Chem.* **2010**, *31(2)*, 455–461. https://doi.org/10.1002/jcc.21334
34. de Bhailís, Á. M.; Chrysochou, C.; Kalra, P. A. Inflammation and Oxidative Damage in Ischaemic Renal Disease. *Antioxidants* **2021**, *10(6)*, 845. https://doi.org/10.3390/antiox10060845
35. Yan, M.-T.; Chao, C.-T.; Lin, S.-H. Chronic Kidney Disease: Strategies to Retard Progression. *Int. J. Mol. Sci.* **2021**, *22(18)*, 10084. https://doi.org/10.3390/ijms221810084
36. Mansour, A. S. Autoregulation: Mediators and Renin–Angiotensin System in Diseases and Treatments. *Future J. Pharm. Sci.* **2023**, *9(1)*, 30. https://doi.org/10.1186/s43094-023-00482-4
37. Ghosh, R.; Alajbegovic, A.; Gomes, A. V. NSAIDs and Cardiovascular Diseases: Role of Reactive Oxygen Species. *Oxid. Med. Cell. Longev.* 2015, *2015(1)*, 536962. https://doi.org/10.1155/2015/536962
38. Kobiec, T.; Otero-Losada, M.; Chevalier, G.; Udovin, L.; Bordet, S.; Menéndez-Maissonave, C.; Capani, F.; Pérez-Lloret, S. The Renin–Angiotensin System Modulates Dopaminergic Neurotransmission: A New Player on the Scene. *Front. Synaptic Neurosci.* **2021**, *13*, 638519. https://doi.org/10.3389/fnsyn.2021.638519
39. Dugbartey, G.J., *Gasotransmitters in Organ Transplantation*. 2024: Springer. https://doi.org/10.1007/978-3-031-48067-6
40. Zhao, S.; Cheng, C. K.; Zhang, C. L.; Huang, Y. Interplay between Oxidative Stress, Cyclooxygenases, and Prostanoids in Cardiovascular Diseases. *Antioxid. Redox Signal.* **2021**, *34(10)*, 784–799. https://doi.org/10.1089/ars.2020.8105
41. Leatherby, R. J.; Theodorou, C.; Dhanda, R. Renal Physiology: Blood Flow, Glomerular Filtration and Plasma Clearance. *Anaesth. Intensive Care Med.* **2021**, *22(7)*, 439–442. https://doi.org/10.1016/j.mpaic.2021.05.003
42. Tsikas, D. Assessment of Lipid Peroxidation by Measuring Malondialdehyde (MDA) and Relatives in Biological Samples: Analytical and Biological Challenges. *Anal. Biochem.* **2017**, *524*, 13–30. https://doi.org/10.1016/j.ab.2016.10.021
43. Tirani, M.; Haghjou, M. Reactive Oxygen Species (ROS), Total Antioxidant Capacity (AOC) and Malondialdehyde (MDA) Make a Triangle in Evaluation of Zinc Stress Extension. *JAPS J. Anim. Plant Sci.* **2019**, *29(4)*.
44. Mazuryk, O.; Gurgul, I.; Oszajca, M.; Polaczek, J.; Kieca, K.; Bieszczad-Żak, E.; Martyka, T.; Stochel, G. Nitric Oxide Signaling and Sensing in Age-Related Diseases. *Antioxidants* **2024**, *13(10)*, 1213. https://doi.org/10.3390/antiox13101213
45. Pérez de la Lastra, J. M.; Andrés Juan, C.; Plou, F. J.; Pérez-Lebeña, E. The Nitration of Proteins, Lipids and DNA by Peroxynitrite Derivatives—Chemistry Involved and Biological Relevance. *Stresses* **2022**, *2(1)*, 53–64. https://doi.org/10.3390/stresses2010005
46. Zhou, X.-Y.; Zhang, J.; Li, Y.; Chen, Y.-X.; Wu, X.-M.; Li, X.; Zhang, X.-F.; Ma, L.-Z.; Yang, Y.-Z.; Zheng, K.-M.; Liu, Y.-D.; Wang, Z.; Chen, S.-L. Advanced Oxidation Protein Products Induce G1/G0-Phase Arrest in Ovarian Granulosa Cells via the ROS-JNK/p38 MAPK-p21 Pathway in Premature Ovarian Insufficiency. *Oxid. Med. Cell. Longev.* **2021**, *2021(1)*, 6634718. https://doi.org/10.1155/2021/6634718
47. Ndrepepa, G. Aspartate Aminotransferase and Cardiovascular Disease—A Narrative Review. *J. Lab. Precis. Med.* **2021**, *6*. https://doi.org/10.21037/jlpm-20-93

48. Jewad, A. M.; Jihad, I. A. Role of Heart Failure in Variation of Serum ALT, AST, ALP, Bilirubin and Electrolytes. *Biochem. Cell. Arch.* **2021**, *21(2)*.

49. Ferrannini, G.; Rosenthal, N.; Hansen, M. K.; Ferrannini, E. Liver Function Markers Predict Cardiovascular and Renal Outcomes in the CANVAS Program. *Cardiovasc. Diabetol.* **2022**, *21(1)*, 127. https://doi.org/10.1186/s12933-022-01558-w

50. Scholz, H.; Boivin, F. J.; Schmidt-Ott, K. M.; Bachmann, S.; Eckardt, K.-U.; Scholl, U. I.; Persson, P. B. Kidney Physiology and Susceptibility to Acute Kidney Injury: Implications for Renoprotection. *Nat. Rev. Nephrol.* **2021**, *17(5)*, 335–349. https://doi.org/10.1038/s41581-021-00394-7

51. Moiseyenko, I.O., et al., *Summary of European recommendations on nephrology.* 2023.

52. Luyckx, V. A.; Rule, A. D.; Tuttle, K. R.; Delanaye, P.; Liapis, H.; Gandjour, A.; Romagnani, P.; Anders, H.-J. Nephron Overload as a Therapeutic Target to Maximize Kidney Lifespan. *Nat. Rev. Nephrol.* **2022**, *18(3)*, 171–183. https://doi.org/10.1038/s41581-021-00510-7

53. Sethi, S.; De Vriese, A. S.; Fervenza, F. C. Acute Glomerulonephritis. *Lancet* **2022**, *399(10335)*, 1646–1663. https://doi.org/10.1016/S0140-6736(22)00461-5

54. Anders, H.-J.; Kitching, A. R.; Leung, N.; Romagnani, P. Glomerulonephritis: Immunopathogenesis and Immunotherapy. *Nat. Rev. Immunol.* **2023**, *23(7)*, 453–471. https://doi.org/10.1038/s41577-022-00816-y

55. He, Y.; Sun, M. M.; Zhang, G. G.; Yang, J.; Chen, K. S.; Xu, W. W.; Li, B. Targeting PI3K/Akt Signal Transduction for Cancer Therapy. *Signal Transduct. Target. Ther.* **2021**, *6(1)*, 425. https://doi.org/10.1038/s41392-021-00828-5